J. Biomedical Science and Engineering, 2014, 7, 792-798
Published Online August 2014 in SciRes. http://www.scirp.org/journal/jbise
http://dx.doi.org/10.4236/jbise.2014.710078

Scientific Research

Optical Probe for Near-Infrared (NIR) Fluorescence Signal Detection with High Optical Performance and Thermal Stability

In Hee Shin, Joo Beom Eom, Jae Seok Park, Hyeong Ju Park, Byeong-Il Lee*

Bio-Photonics Research Center, Korea Photonics Technology Institute, Gwangju, Korea
Email: ihshin@kopti.re.kr, jbeom@kopti.re.kr, jspark@kopti.re.kr, hj202@kopti.re.kr, *bilee@kopti.re.kr

Received 6 June 2014; revised 22 July 2014; accepted 1 August 2014

Abstract

We propose a new optical probe for near-infrared (NIR) fluorescence signal detection with high optical performance and thermal stability. The optical probe is composed of an optical source part for efficient excitation of NIR fluorescence signal, a heat dissipation part for stable operation of the NIR fluorescence probe, and an optical detection part for efficient detection of NIR fluorescence signal. From a simulation by use of an optical simulation tool, Light Tools™, we could confirm that the optical probe has optical propagation efficiency of 79.6% in case of using a circular detector with 20 cm in diameter located at 20 cm in distance from the optical source. From a measurement of temperature variation of the optical probe, we could also confirm that the optical probe has thermal stability with a standard deviation of 2.19˚C under room temperature condition. Finally, from an evaluation of fluorescence image quality, we could confirm that an optical noise which can bring on by overlapped band between optical spectrum of the optical source for fluorescence excitation and optical spectrum of the emitted fluorescence signal decreased effectively in the optical probe.

Keywords

Near-Infrared, Fluorescence, LEDs, Liquid Circulation Module

1. Introduction

NIR fluorescence imaging has been used to improve sentinel lymph node (SLN) mapping in breast cancer patients, to assess the extent of colorectal metastases during curative-intended surgery and so on because NIR has relatively low absorption and scattering rates in hemoglobin, water and lipid [1]-[8]. LED based light sources

*Corresponding author.

How to cite this paper: Shin, I.H., Eom, J.B., Park, J.S., Park, H.J. and Lee, B.-I. (2014) Optical Probe for Near-Infrared (NIR) Fluorescence Signal Detection with High Optical Performance and Thermal Stability. *J. Biomedical Science and Engineering*, **7**, 792-798. http://dx.doi.org/10.4236/jbise.2014.710078

have been used in image guided surgery, and in NIR fluorescence-guided surgery because of characteristics of long working distance, computer control, and spectral confinement (typical full width at half maximum, FWHM, 50 μm) and so on. Especially, LEDs come into the spotlight as light sources for medical use because LEDs with high power (more than 1 watt) have been developed recently. Actually, LEDs have been used in NIR fluorescence imaging system such as FLARE^{TM} (Fluorescence-assisted resection and exploration) image guided surgery system and PDE^{TM} (Photodynamic eye, Hamamatsu) [9]-[11]. However, although optical power of LEDs has been improved, LEDs still have weaknesses to be considered in medical application such as heat, broad divergence angle, relatively broad spectrum and so on.

In this paper, we propose an optical probe for NIR fluorescence signal detection with high optical performance and thermal stability by making up for the weakness and strengthening the strength of LEDs with high optical power in the optical probe.

2. Methods and Results

2.1. An Array of LEDs

Although LEDs with high optical power were developed recently, optical power of single LED is not still sufficient as a light source for medical purposes because of large divergence angle of LEDs. Therefore, an array of LEDs was introduced to overcome insufficient optical power as shown in **Figure 1(a)**. The array of LEDs is composed of 16 LEDs (SP95MR-D2-1W-780, center wavelength: 780 nm, full width at half maximum: 30 nm, Innolight Co.) with each 1 W optical power. 780 nm was selected as each LED's wavelength because ICG (Daiichi Sankyo Propharma Co.) which was used to evaluate characteristics of the optical probe has maximum excitation characteristic at 780 nm wavelength. LEDs were not installed in the midmost because the midmost was regarded as a position of a CCD camera (Guppy Pro 031B, Allied Vision Technology Co.) to detect fluorescence signal.

2.2. A Mirror and Lenses for Efficient Propagation of Light Radiated from the Array of LEDs

The array of LEDs improved optical intensity as a light source for medical purposes. However, the array of LEDs has still insufficient optical propagation efficiency because each LED in the array of the LEDs has broad divergence angle (generally half angle of LED is about 120˚). A mirror to improve optical propagation efficiency of light radiated from the array of LEDs was introduced as shown in **Figure 1(b)**. The mirror which has reflective surfaces of parabolic shape was installed in front of the array of LEDs. Also, 16 MgF_2 coated lenses (#45-209, Edmund Optics) were introduced to improve optical propagation efficiency of light radiated from the array of LEDs. The lenses were installed in front of each reflection surface of the mirror.

Propagation efficiency of light radiated from the optical probe which is composed of the array of LEDs, the mirror and the lenses was simulated by use of Light Tools^{TM} (Optical Research Associates, USA). Propagation efficiency of light radiated from the array of LEDs could not be measured because we didn't have an optical

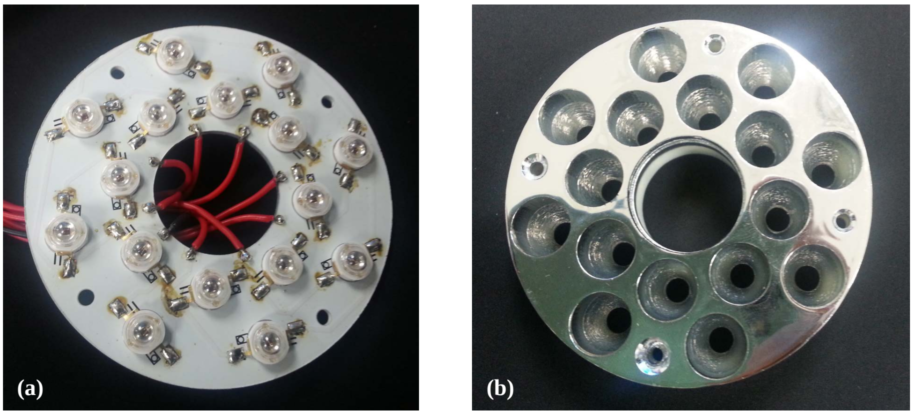

Figure 1. Pictures of (a) the array of LEDs and (b) the mirror for the array of LEDs.

power meter with large active area (about 30cm in diameter). So, we replaced the propagation efficiency measurement with optical simulation. In the simulation, a circular detector with 20 cm in diameter was considered as a comparison target of a human breast. **Figure 2** shows simulation results of the optical intensity which was radiated from the optical probe. Also, **Table 1** shows simulation results of the propagation efficiency of the optical probe system. **Figure 3** shows the intensity variation of light to come into the detector according to distance variation from the optical probe. From the **Figure 3**, we could confirm that 12.73 watt out of total light power, 16 watt can propagate into the circular detector with 20 cm in diameter located at 20 cm in distance from the optical probe by use of the array of LEDs, the mirror and the collimating lenses (about 79.6% optical propagation efficiency). In this case, 20 cm in distance from the optical probe was considered as a minimum distance for efficient fluorescence detection in clinical application.

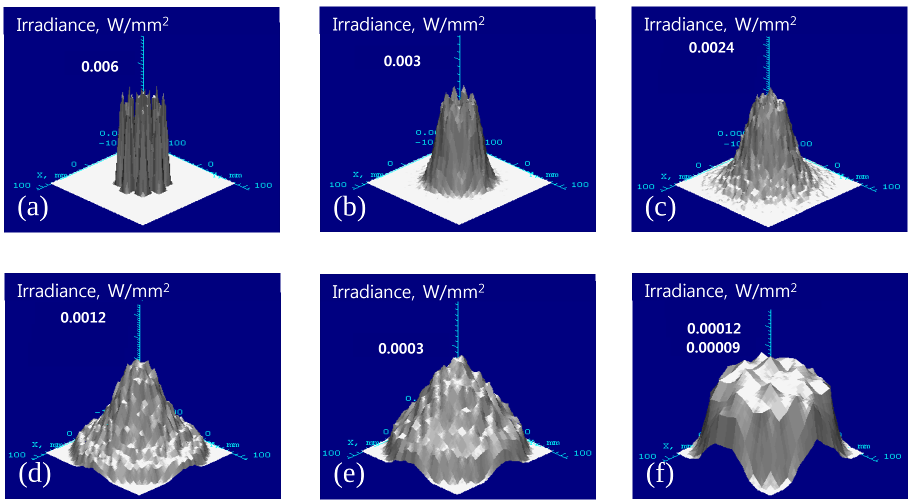

Figure 2. Simulation results on propagation of the optical probe system at (a) 0 cm (b) 5 cm (c) 10 cm (d) 20 cm (e) 40 cm and (f) 80 cm distance from the probe.

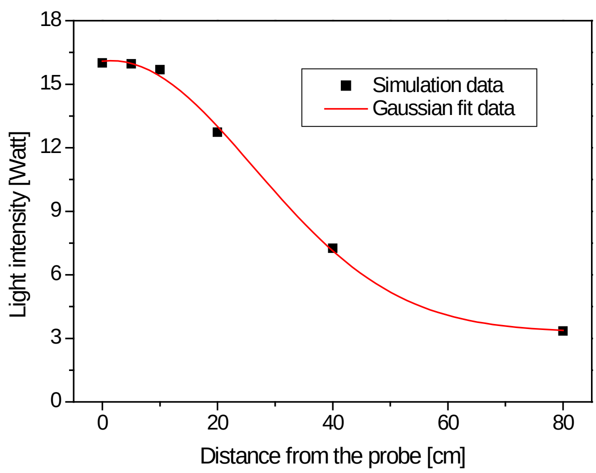

Figure 3. The intensity variation of incident light into the detector.

Table 1. Propagation efficiency of the optical probe system.

Distance from the probe (cm)	0	5	10	20	40	80
Optical power come into the detector (Watt)	16	15.96	15.68	12.73	7.25	3.35
Propagation efficiency of the LEDs (%)	100	99.8	98	79.6	45.3	20.9

2.3. A Liquid Circulation Module for Heat Dissipation of the Array of LEDs

The array of LEDs generates much heat because the array of LEDs is composed of 16 high-power LEDs. The heat generated from the array of LEDs degrades image quality of the CCD camera because the array of LEDs is in contact with the CCD camera as shown in **Figure 4(a)**. So, a liquid circulation module was introduced to cool down heat generated from the array of LEDs. **Figure 5** shows the liquid circulation module. Antifreeze was injected into an inlet through a polymer tube and then antifreeze was released from an outlet after circulation in the liquid circulation module. Under operation of the array of LEDs, temperature on three regions (region 1, 2, and 3 in **Figure 4(a)**) of the optical probe was measured by an infrared thermometer (TK-307A, Tae Kwang Electronics Co.). **Figure 6** shows the temperature variation of the optical probe during operation of the liquid

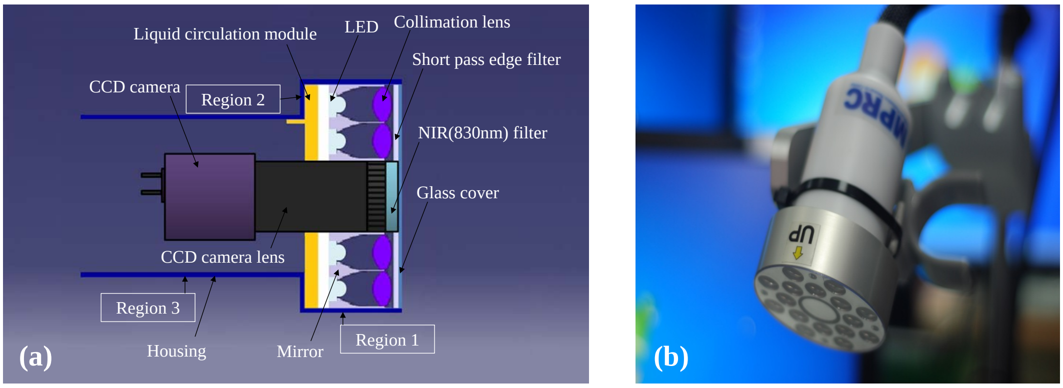

Figure 4. (a) Block diagram and (b) picture of the optical probe for NIR fluorescence.

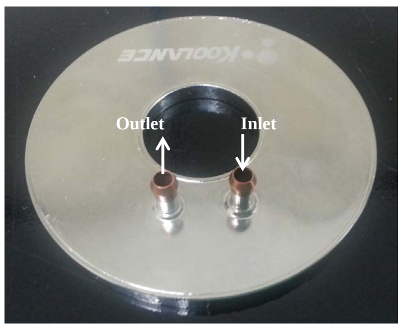

Figure 5. Liquid circulation module for heat dissipation of the array of LEDs.

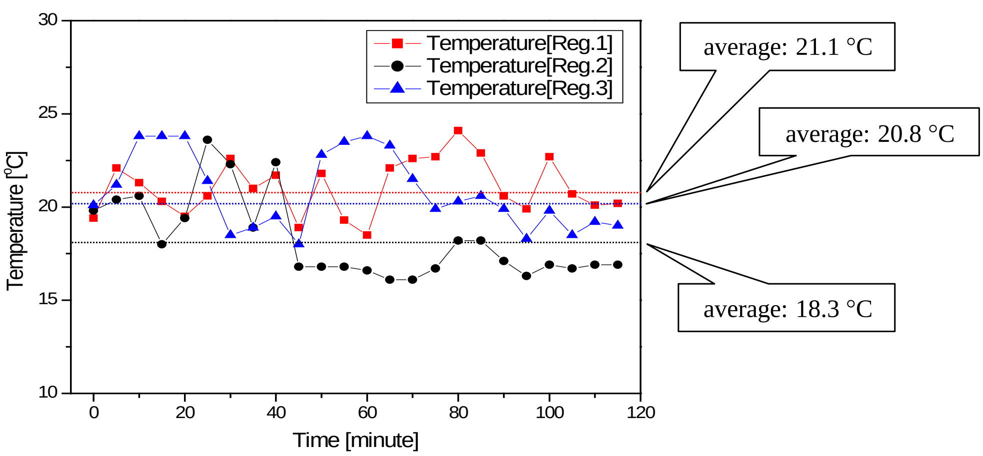

Figure 6. Temperature variation of the probe during operation of the liquid circulation module.

circulation module and operation of the array of LEDs. **Table 2** shows temperature variation data of the optical probe during operation of the liquid circulation module and operation of the array of LEDs. From **Figure 6** and **Table 2**, we could confirm the liquid circulation module is very efficient to dissipate the heat generated from the array of LEDs.

2.4. A Short-Pass Edge Filter for Optical Noise Elimination of the Array of LEDs

Generally LEDs have broad spectral width (about 50 nm, Full Width at Half Maximum) unlike laser diodes (LDs). Although LED used as a light source for fluorescence excitation has a peak at 780 nm wavelength, it has wavelength components of 800 - 830 nm band. The wavelength components can result in optical noise in fluorescence imaging because wavelength components of 800 - 830 nm band may be detected by CCD camera after reflection by sample or other objects. To confirm the optical noise problem, ICG fluorescence imaging experiment was conducted with 740 nm LEDs (SP95MR-D2-1W-740, center wavelength: 740 nm, full width at half maximum: 30 nm, Innolight Co.) and 780 nm LEDs (SP95MR-D2-1W-780, center wavelength: 780 nm, full width at half maximum: 30 nm, Innolight Co.). We controlled optical power of 740 nm LEDs and 780 nm LEDs identical, respectively and checked the optical power with the optical power meter (PKIT-07-01, Newport). After check of equality in optical power of 740 nm LEDs and 780 nm LEDs, we put a piece of gauze including a coated part and a control part uncoated with ICG solution (1.25 μg/ml) as shown in **Figure 7(a)** on the optical power meter. **Figure 7(b)** and **Figure 7(c)** show the fluorescence images of ICG when 740 nm LEDs and 780 nm LEDs were used as the excitation light source, respectively. From **Figure 7(b)**, we could confirm that fluorescence image with less optical noise could be acquired when 740 nm LEDs was used as the excitation light source and that fluorescence signals of ICG by excitation of 740 nm LEDs are very weak because ICG has maximum excitation characteristic at 780 nm wavelength. From **Figure 7(c)**, we could confirm that 830 nm

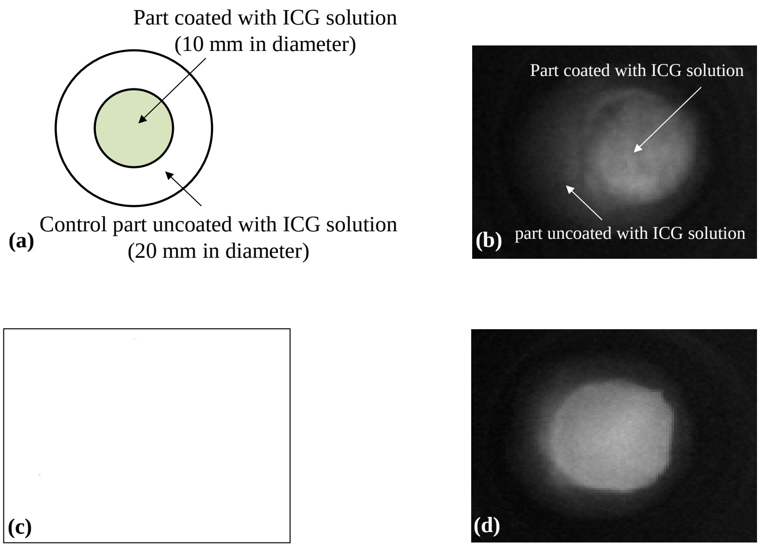

Figure 7. (a) A piece of gauze to test fluorescence signals of ICG (b) fluorescence image by 740 LEDs (c) fluorescence image by 780 LEDs and (d) fluorescence image by 780 LEDs with a short-pass edge filter.

Table 2. Temperature variation data of the optical probe system during operation of the liquid cooling module under operation of the array of LEDs.

	Region 1	Region 2	Region 3
Minimum value (˚C)	18.5	16.1	18.0
Maximum value (˚C)	24.1	23.6	23.8
Standard deviation (˚C)	1.47	2.19	2.02

light emitted from 780 nm LEDs was detected by the CCD camera and acted as optical noise in fluorescence imaging. To solve the optical noise problem, a short-pass edge filter (Edge wavelength: 820 nm, Green Optics, Korea) was arranged in front of 780 nm LEDs. **Figure 7(d)** shows the fluorescence image of ICG when 780 nm LEDs with the short-pass edge filter was used as the excitation light source. From **Figure 7(d)**, we could confirm that 830 nm light emitted from 780 nm LEDs was effectively blocked by the short-pass edge filter and that fluorescence signals of ICG by excitation of 780 nm LEDs improved compared with those by excitation of 740 nm LEDs. In case of use of the short-pass edge filter, contrast (C) which is defined as Equaiton (1) increased from 0 to 0.89 in comparison with case of no use of the short-pass edge filter.

$$C = \frac{I_{FS} - I_{BS}}{I_{FS} + I_{BS}} \tag{1}$$

where I_{FL} is intensity of fluorescence signal at the part coated with ICG solution and I_{BS} is intensity of background signal at the control part uncoated with ICG solution in **Figure 7**.

3. Conclusion

In this paper, we propose an optical probe for NIR fluorescence signal detection with high optical performance and thermal stability. Propagation efficiency of light in the optical probe was improved by use of an array of LEDs, a mirror, and collimating lenses. Propagation simulation results of the optical probe showed propagation efficiency of 79.6% about a circular detector with 20 cm in diameter located at 20 cm in distance from the optical probe. Heat generated from the optical probe was efficiently dissipated by use of a liquid circulation module. Actually, temperature of the optical probe was maintained below 25˚C. Finally, optical noise of the optical probe which occurs by broad spectral width of LEDs was efficiently eliminated by use of the short-pass edge filter. Therefore, we believe that our optical probe for NIR fluorescence signal detection can provide excellent NIR fluorescence images with high quality in applications of clinical fields.

Acknowledgements

This work was supported by the National Research Foundation of Korea (NRF) funded by the Ministry of Science, ICT & Future Planning (2013-035981).

References

[1] Hutteman, M., Mieog, J.S.D., van der Vorst, J.R., Liefers, G.J., Putter, H., Löwik, C.W.G.M., Frangioni, J.V., van de Velde, C.J.H. and Vahrmeijer, A.L. (2011) Randomized, Double-Blind Comparison of Indocyanine Green with or without Albumin Premixing for Near-Infrared Fluorescence Imaging of Sentinel Lymph Nodes in Breast Cancer Patients. *Breast Cancer Research and Treatment*, **127**, 163-170. http://dx.doi.org/10.1007/s10549-011-1419-0

[2] Shin, I.H., Kim, S.K., Eom, J.B., Park, J.S., Park, H.J., Park, I.-K. and Lee, B.-I. (2013) Novel Imaging System for Positioning of the Indocyanine Green (ICG) Target; Visible Projection of the Near-Infrared Fluorescence Image. *Journal of Biomedical Science and Engineering*, **6**, 896-900. http://dx.doi.org/10.4236/jbise.2013.69109

[3] van der Vorst, J.R., Hutteman, M., Mieog, J.S.D., de Rooij, K.E., Kaijzel, E.L., Löwik, C.W.G.M., Putter, H., Kuppen, P.J.K., van de Velde, C.J. and Vahrmeijer, A.L. (2012) Near-Infrared Fluorescence Imaging of Liver Metastases in Rats Using Indocyanine Green. *Journal of Surgery Research*, **174**, 266-271. http://dx.doi.org/10.1016/j.jss.2011.01.009

[4] Miego, J.S.D., Hutteman, M., van der Vorst, J.R., Kuppen, P.J.K., Que, I., Dijkstra, J., Kaijzel, E.L., Prins, F., Lowik, C.W.G.M., Smit, V.T.H.B.M., van de Velde, C.J.H. and Vahrmeijer, A.L. (2011) Image-Guided Tumor Resection Using Real-Time Near-Infrared Fluorescence in a Syngeneic Rat Model of Primary Breast Cancer. *Breast Cancer Research and Treatment*, **128**, 279-689. http://dx.doi.org/10.1007/s10549-010-1130-6

[5] Troyan, S.L., Kianzad, V., Gibbs-Strauss, S.L., Gioux, S., Matsui, A., Oketokoun, R., Ngo, L., Khamene, A., Azar, F. and Frangioni, J.V. (2009) The FLARE Intraoperative Near-Infrared Fluorescence Imaging System: A First-in-Human Clinical Trial in Breast Cancer Sentinel Lymph Node Mapping. *Annals of Surgical Oncology*, **16**, 2943-2952. http://dx.doi.org/10.1245/s10434-009-0594-2

[6] Murawa, D., Hirche, C., Dresel, S. and Hunerbein, M. (2009) Sentinel Lymph Node Biopsy in Breast Cancer Guided by Indocyanine Green Fluorescence. *British Journal of Surgery*, **96**, 1289-1294. http://dx.doi.org/10.1002/bjs.6721

[7] Sevick-Muraca, E.M., Sharma, R., Rasmussen, J.C., Marshall, M.V., Wendt, J.A., Pham, H.Q., Bonefas, E., Houston, J. P., Sampath, L., Adams, K.E., Blanchard, D.K., Fisher, R.E., Chiang, S.B., Elledge, R. and Mawad, M.E. (2008) Im-

aging of Lymph Flow in Breast Cancer Patients after Microdose Administration of a Near-Infrared Fluoro-Phore: Feasibility Study. *Radiology*, **246**, 734-741. http://dx.doi.org/10.1148/radiol.2463070962

[8] Tagaya, N., Yamazaki, R. and Nakagawa, A. (2008) Intraoperative Identification of Sentinel Lymph Nodes by Near-Infrared Fluorescence Imaging in Patients with Breast Cancer. *American Journal of Surgery*, **195**, 850-853. http://dx.doi.org/10.1016/j.amjsurg.2007.02.032

[9] Gioux, S., Kianzad, V., Ciocan, R., Gupta, S., Oketokoun, R. and Frangioni, J.V. (2009) High Power, Computer-Controlled, LED-Based Light Sources for Fluorescence Imaging and Image-Guided Surgery. *Molecular Imaging*, **3**, 156-165.

[10] Gioux, S., Choi, H.S. and Frangioni, J.V. (2010) Image-Guided Surgery Using Invisible Near-Infrared Light: Fundamentals of Clinical Translation. *Molecular Imaging*, **9**, 237-255.

[11] Miwa, M. (2008) The Principle of ICG Fluorescence Method. *The Open Surgical Oncology Journal*, **2**, 26-28. http://dx.doi.org/10.2174/1876504101002020026


Advances in Bioscience and Biotechnology
Applied Mathematics
American Journal of Plant Sciences
Creative Education
Engineering
HEALTH
Journal of Computer and Communications
Journal of Modern Physics
Journal of Environmental Protection
Agricultural Sciences
Food and Nutrition Sciences
Psychology
Natural Science
Modern Economy
Journal of Cancer Therapy
American Journal of Analytical Chemistry